Study on Fault Diagnosis in a Spacecraft Propulsion System

Kazushi ADACHI[1], Samir KHAN[2], Kohji TOMINAGA[3], Noriyasu OMATA[4], Seji TSUTSUMI[5], and Taiichi NAGATA[6]

[1,2] *Department of Aeronautics and Astronautics, The University of Tokyo, Tokyo, 113-0033, Japan*
adachi-kazushi@g.ecc.u-tokyo.ac.jp
kviz3671@g.ecc.u-tokyo.ac.jp

[3,4,5,6] *Japan Aerospace Exploration Agency, Tsukuba, Ibaraki, 305-8505, Japan*
tominaga.kohji@jaxa.jp
omata.noriyasu@jaxa.jp
tsutsumi.seiji@jaxa.jp
nagata.taiichi@jaxa.jp

ABSTRACT

The propulsion system in a spacecraft is an important subsystem for orbit transfer and attitude control. A fast and accurate fault diagnosis system contributes to the safety of the entire system. As the system becomes more complex, identifying faults, their locations, and root causes becomes increasingly difficult. This study utilized Principal Component Analysis (PCA) and feature optimization with Fast Fourier Transform (FFT) analysis using greedy algorithm to achieve fault diagnosis systems for spacecraft to replace the current operation based on the expert knowledge. By applying PCA to simulation data for the faults were successfully detected and their locations and root causes identified.

1. INTRODUCTION

In recent years, due to the space development beyond Earth's orbit, such as the lunar Gateway and Mars exploration, there is a demand for the development of orbital transfer vehicles capable of transporting supplies to such remote locations. In such remote missions, due to communication delays between ground stations on Earth and spacecraft, autonomous systems that do not rely on human decision become necessary. In particular, the propulsion system in a spacecraft is an important subsystem for orbit transfer and attitude control. Therefore, a fast and accurate fault diagnosis system contributes to the safety of the entire system.

In previous research, anomaly detection, isolation, and diagnosis methods based on expert knowledge, such as expert systems, have been the focus of attention. These approaches offer the advantage of diagnosing anomalies in more detail compared to the classical red-line judgement (Yairi, 2017). However, the preparation of knowledge-based systems requires enormous time and human resource costs. As the target systems become more complex, these costs increase even further. On the other hand, anomaly detection systems based on data-driven methods that discover general rules and patterns from large amounts of data have gained attention in various fields. An advantage of this approach is that it does not require complete expert knowledge beforehand. However, data-driven approaches require an enough amount of data to be collected in advance. Due to the high testing costs of spacecraft, data collection through physical experiments is challenging.

In this study, a low computation cost machine learning method is proposed for realizing on-board fault diagnosis using the data generated by a physical simulation model for the supply piping of spacecraft propulsion systems and demonstrate the effectiveness of the proposed approach. Specifically, the evaluation of an on-board anomaly fault diagnosis system using principal component analysis (PCA) is conducted using internal pressure data of the spacecraft propulsion system obtained from the simulation model created by Japan Aerospace Exploration Agency (JAXA), with appropriate preprocessing and feature extraction applied.

The remaining sections of this paper are organized as follows. Section 2 briefly introduces the previous methods of anomaly detection and diagnosis for various systems as well as the propulsion systems of spacecraft. Section 3 describes the physical simulation model built by JAXA and the data generated by using it. Section 4 introduces the feature extraction of the data and the fundamental concepts of the proposed method. Section 5 resent and discuss the results of the proposed method. Section 6 presents some concluding remarks.

2. RELATED WORK

In this section, an introduction to the previous research are provided. Specifically, data-driven anomaly detection method related to the approach used in this study is discussed. Additionally, research on anomaly detection systems for spacecraft are presented. The relationships and differences between each study and this research are discussed.

2.1. Anomaly Detection by Using Data-Driven Approach

Hoan and Nguye (2018) builds a PCA-based anomaly detection method for IoT networks. In anomaly detection for IoT networks, a low computational cost algorithm is desirable for rapidly detecting anomalies in high-dimensional and enormous amounts of data. The authors introduced a new distance calculation method to further reduce the computational cost of PCA and achieved high-precision anomaly detection model with a small number of computers. However, IoT anomalies include those related to performance (network failures, changes in link traffic, flash crowd, etc.) and security (attacks such as denial of service attacks, network scans, etc.), and this study is limited to anomaly detection without the capability to isolate and diagnose the root causes. In contrast, the proposed research demonstrates not only anomaly detection but also the ability to isolate and diagnose the root causes of anomalies using PCA.

With the development of "deep learning" method, such techniques have also been applied to anomaly detection in spacecraft. Hundman, Constantinou, Laporte, Colwell, and Soderstrom (2018) demonstrated the ability to detect anomalies with high accuracy by applying non-parametric threshold processing to Long Short-Term Memory (LSTMs) for learning and prediction on telemetry data from the orbital satellite (SMAP) and Mars rover (Curiosity). However, while these deep learning-based anomaly detection systems can be operated in ground stations with abundant computational resources, their execution on-board is challenging due to computational resource and memory limitations. In this study, more relatively low computational cost and higher feasibility for on-board execution method for anomaly detection, isolation and diagnosis is proposed.

2.2. Anomaly Detection for Spacecraft Propulsion System

JAXA focuses on health monitoring systems for highly safe propulsion systems, aiming for the realization of next-generation orbital transfer vehicles. For example, Kawatsu, Noumi, Ishihama, and Nagata (2020) focused on pressure propagation called "water hammer" in the piping system of spacecraft propulsion systems and proposed an approach to fault diagnosis method based on the frequency domain dynamic response. This method demonstrated the possibility of building a health management system with high reliability and robustness using only general pressure sensor information rather than traditional system based on attitude information. Additionally, it was shown that by building a physical model of the propulsion system in a simulation environment, it is possible to generate datasets of failure scenarios that are difficult to obtain in physical experiments. In this study, an anomaly detection method using data generated from such physical models is proposed.

Tominaga, Fujii, Nagata, Wada, Hisada, Kawatsu, and Kasai (2022) used lightweight and multi-channel Fiber Bragg Gratings sensors (Vohra, 1999) to measure pressure fluctuations in supply piping caused by water hammer through the physical experiments. They demonstrated the feasibility of anomaly detection using the mean squared error of the Frequency Response Function (FRF) obtained from any two arbitrary measurement points during normal and abnormal operation. However, difficulty still exists in the determination of threshold to separate fault from normal condition, which results in degrading the robustness of the method. In addition, diagnosis of the root cause of the fault was still a challenge. In this study, a method is proposed that not only detects anomalies but also enables the separation of abnormal locations and the diagnosis of their causes.

3. PROBLEM STATEMENT

In this section, the dataset used in this study is introduced. The dataset was generated from a fluid simulation model created by JAXA (Tominaga, 2023) using SimulationX® (SimulationX, 2023), which supports Modelica-based (Modelica, 2023) modeling and simulation capability. The diagram of the model is shown in Figure 1. Note that the propulsion system in this study is simplified compared to an actual spacecraft propulsion system. The fluid is driven from the left upstream side to the right downstream side and the water is pressurized up to 2.0 MPa. Here, SV is a solenoid valve that is opened and closed three times with a duty ratio of 100 ms open, 300 ms close, and an error range is 1 ms. P is a pressure measurement point that the pressure data at the point is obtained. BV and BP are accumulators for simulating bubble localization, and the amount of the bubble injected at this point can be controlled. As an example, Figure 2 shows the pressure fluctuations at P1 under normal conditions. The reason that the timing of open and close does not match the pressure fluctuations is that the pressure fluctuations generated at the solenoid valve position take time to propagate. The large pressure fluctuations called water hammer occurs when the valve is closed. In this study, the water hammers followed by acoustic modes generated inside the propulsion system were used for the features of fault diagnosis system. The data was divided into three independent datasets for each water hammer to increase the amount of data. Detail of the data set used in this study is summarized in Table 1. There are 18 normal data (Case1). Assuming one of the valve failures,

there are 3 fault data (Case2-5) for each of the valves SV1 to SV4, remaining valve are closed. Additionally, there are 3 abnormal data (Case6-13) each for the bubbles added at one of BP1 and BV1 to BV7.

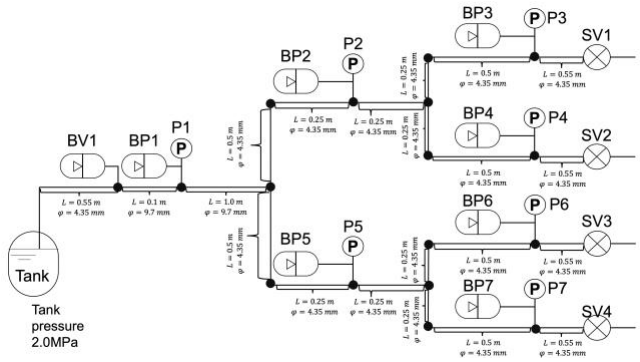

Figure 1. The diagram of the simulation model of a spacecraft propulsion system.

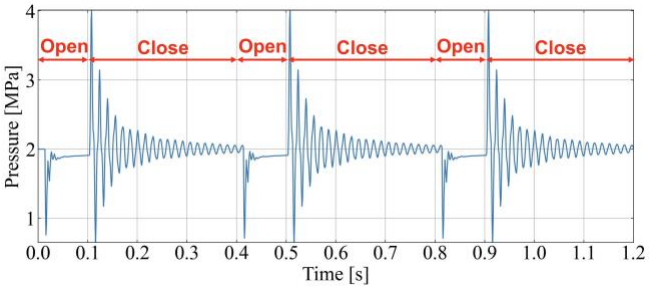

Figure 2. Time-series result at P1 under normal condition.

Table 1. List of datasets.

Case name	Condition	Number of data
Case 1	Normal	18
Case 2	Fault in SV1	3
Case 3	Fault in SV2	3
Case 4	Fault in SV3	3
Case 5	Fault in SV4	3
Case 6	Bubble anomaly at BV1	3
Case 7	Bubble anomaly at BP1	3
Case 8	Bubble anomaly at BP2	3
Case 9	Bubble anomaly at BP3	3
Case 10	Bubble anomaly at BP4	3
Case 11	Bubble anomaly at BP5	3
Case 12	Bubble anomaly at BP6	3
Case 13	Bubble anomaly at BP7	3

4. METHODOLOGY

In this section, the feature extraction of the data and the fundamental concept of the proposed method is introduced.

4.1. Feature Extraction

In data-driven methods, including PCA used in this study, the feature extraction that extracts variables that well represent the differences between normal and abnormal data is essential to improve the model. According to Tominaga et al. (2022), it is known that there are significant differences in the frequency domain between normal and abnormal data in pressure fluctuations caused by water hammer. Therefore, in this study, data extracted by Fast Fourier Transformation (FFT) was used as features. Additionally, basic statistical features were extracted from the time-series signal data. Table 2 shows the candidate features. To optimize these features, a greedy algorithm was used for feature optimization. Specifically, for all possible combinations of these features, the area under the curve (AUC) based on the anomaly scores introduced in the following chapter was calculated. The optimal features were determined as those that maximize this AUC. By performing a greedy feature optimization for the features, a total of three features were finally extracted from the seven sensors P1 to P7: the standard deviation of the time-series data, and the peak frequency values at 0-100 Hz and 100-150 Hz ranges in FFT. Thus, the total number of features obtained is 21.

Table 2. List of candidate features.

	Feature name
Statistical	Mean
	Standard deviation
	Maximum
	Minimum
	Skewness
	Kurtosis
FFT	Peak amplitude at 0-100Hz
	Peak frequency at 0-100Hz
	Peak amplitude at 100-150Hz
	Peak frequency at 100-150Hz
	Peak amplitude at 150-200Hz
	Peak frequency at 150-200Hz
	Peak amplitude at 200-300Hz
	Peak frequency at 200-300Hz
	Peak amplitude at 300-500Hz
	Peak frequency at 300-500Hz

4.2. Anomaly Detection Using PCA

With the notable advancements in deep learning in recent years, its application in the field of health management is gathering attention (Khan and Yairi ,2018). However, the performance of deep learning models is heavily dependent on the quality and quantity of the data. Moreover, when considering the application of deep learning to spacecraft using FPGA (Field-Programmable Gate Array), there is a risk associated with the computational complexity of the model, as it remains uncertain whether the deep learning system would function adequately. In this work, a fault diagnosis algorithm utilizing Principal Component Analysis (PCA) is proposed as a potential solution to develop a lightweight method that is independent of data quality or quantity and does not impose significant computational requirements. Principal Component Analysis (PCA) is one of the dimensionality reduction methods, which finds the axes called principal component that maximize the overall variance from the original high-dimensional data. The variation in the data can be obtained with fewer dimensions using principal components while minimizing the loss of information (Wold, et al., 1987). In PCA anomaly detection, only normal data is used as training data to determine the normal subspace. The "anomaly score" of the test data can be evaluated by calculating the error (reconstruction error) between the original data and the reconstructed data using the learned subspace. Considering the mapping to q -dimensional ($q < p$) space from the normalized training dataset $\boldsymbol{X_{train}} = [\boldsymbol{x_1}, \boldsymbol{x_2} \dots \boldsymbol{x_p}]$ with p features. The projection matrix $\boldsymbol{W} = [\boldsymbol{w_1}, \boldsymbol{w_2} \dots \boldsymbol{w_q}]$, consisting of the eigenvectors corresponding to the top q eigenvalues $\lambda_1, \lambda_2 \dots \lambda_q$ of the variance-covariance matrix obtained from $\boldsymbol{X_{train}}$, is defined. Here, the k-th column of W is the k-th principal component of $\boldsymbol{X_{train}}$. The vector $\boldsymbol{y_{i,test}}$ in the lower-dimensional space of the i-th test data $\boldsymbol{x_{i,test}}$ in the test dataset $\boldsymbol{X_{test}}$ is calculated as Eq. (1).

$$\boldsymbol{y_{i,test}} = \boldsymbol{W^T x_{i,test}} \tag{1}$$

The reconstructed data $\hat{\boldsymbol{x}}_{\boldsymbol{i,test}}$ is calculated as Eq. (2).

$$\hat{\boldsymbol{x}}_{\boldsymbol{i,test}} = \boldsymbol{W y_{i,test}} = \boldsymbol{W W^T x_{i,test}} \tag{2}$$

By calculation of the error $\boldsymbol{e_i}$ between the original data $\boldsymbol{x_{i,test}}$ and the reconstructed data $\hat{\boldsymbol{x}}_{\boldsymbol{i,test}}$, The anomaly score of each data point from the normal subspace is obtained as Eq. (3).

$$\boldsymbol{e_i} = \left\| \boldsymbol{x_{i,test}} - \hat{\boldsymbol{x}}_{\boldsymbol{i,test}} \right\|^2 \tag{3}$$

Here, $\|\cdot\|^2$ represents the Euclidean norm. If the test data is abnormal, it is expected that the reconstructed data will be significantly different from the original data, resulting in a larger error $\boldsymbol{e_i}$.

The importance of the principal components is evaluated as the "contribution ratio", α [%]. The contribution ratio of the kth principal component is calculated as Eq. (4).

$$\alpha = (\lambda_k / \sum_{i=1}^{p} \lambda_i) \times 100 \tag{4}$$

4.3. Fault Diagnosis Using PCA

PCA can be applied as supervised learning method for fault diagnosis. The training data $\boldsymbol{X_{train}} = [\boldsymbol{x_1}, \boldsymbol{x_2} \dots \boldsymbol{x_p}]$ differs from the one in the previous section, as it includes abnormal and fault data. It is assumed that PCA can calculate principal components that cluster normal, abnormal and fault cases in a low-dimensional space. By checking which cluster in the low-dimensional space the i-th test data $\boldsymbol{x_{i,test}}$ maps to nearby, it is possible to determine which abnormal case the test data corresponds to. A schematic diagram is shown in Figure 3. This enables the identification of the known anomaly locations and causes. Furthermore, data that do not belong to any known clusters can be considered as unknown cases.

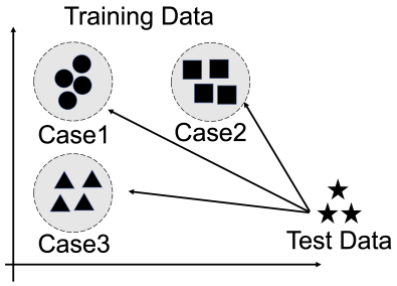

Figure 3. Schematic diagram of PCA clustering for anomaly isolation and diagnosis in two dimensions.

5. Result and Discussion

In this section, results obtained from two experiments, anomaly detection, isolation and diagnosis are presented.

5.1. Anomaly Detection Using Reconstruction Error from PCA

In this experiment, 12 normal data was used for training data, and the remaining 42 data was used for test data. Considering the contribution ratio of PCA, the dimension was set to $q = 2$. At this time, the contribution ratio α was 99.1%. The reconstruction errors for each test data were calculated and the averages for each case are shown in Figure 4. The error bars represent the variance for each case. From the figure, the reconstruction error for Case 1, the normal case, is relatively smaller than that for the other anomaly and fault cases. This is because PCA appropriately learned the normal subspace during training, resulting in a better reconstruction for the test data in Case 1, while the reconstructions for the other cases were significantly different from the original data. Furthermore, when comparing the reconstruction errors for the anomaly and fault cases, the reconstruction errors for Case 6 and Case 13 are relatively small, and both have similar average values.

The reason for the smaller reconstruction errors is that the pressure fluctuations in these cases were similar to the normal case, as the bubble injection locations were farthest from downstream locations where water hammer occurs. The similarity in error values is presumed to be attributed to the relatively close distance between BV1 and BP1 compared to the distances of other accumulators, resulting in similar pressure fluctuations. The important point to note in these results is that the number of test data points used, 6 for Case 1 and 3 for the others, is small and there is a possibility that the distribution of normal, abnormal, and fault cases has not been adequately captured. This issue can be improved by generating more data points with a broader distribution through simulation and using them for training and test data.

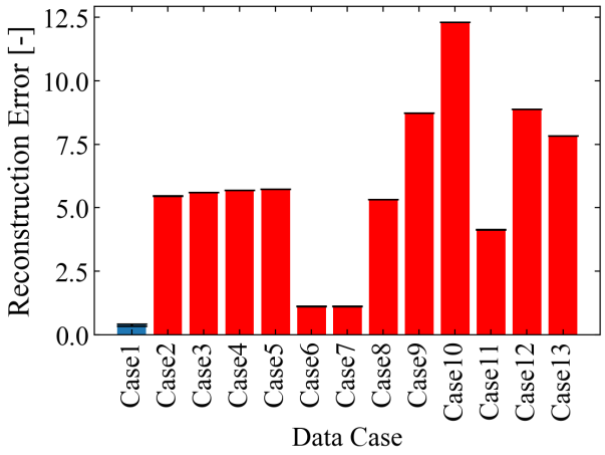

Figure 4. Result of reconstruction error for each cases using PCA.

5.2. Fault Diagnosis by Plotting into Two Dimensions

In this experiment, 12 normal data and 2 anomaly or fault data was used for training data, and other 18 data is used for test data. Figure 6(a) shows the results of plotting the training and test data in two dimensions, using the first principal component (PC1) as the X-axis and the second principal component (PC2) as the Y-axis. The training data is represented with dotted lines, while the test data is shown with solid lines. The test data is displayed larger than training data. Figure 6(b) shows only the SV fault data and Figure 6(c) shows only the bubble anomaly data in two dimensions. From Figure 6(a), normal data (Case1) forms clusters in the range of PC1: -2.0 to -1.7 and PC2: -2.1 to -2.9, SV fault data (Cases 2-5) in the range of PC1: -3.4 to -3.2 and PC2: -3.6 to -3.3, and bubble anomaly data (Cases 6-13) in the range of PC1: -2.5 to -7.5 and PC2: 1.2 to -1.2. Furthermore, Figures 6(b) and 6(c) show that the clusters are formed for each abnormal location of SV fault and each abnormal location of bubble anomalies. However, in Figure 6(c), the positions of Cases 6 and 7 are very close, and the clusters are not clearly separated compared to other cases. This is thought to be the similar reason, which is explained in previous section, the bubble injection points were farthest from downstream locations where water hammer occurs, resulting in pressure fluctuations similar to normal cases, and the distances between BV1 and BP1 were relatively close compared to other accumulators, resulting in similar pressure fluctuations. As with the previous section, important point of this result is that the number of test data points used is small and there is a possibility that the distribution of normal, abnormal, and fault cases has not been adequately captured. This issue can also be improved by generating more data points with a broader distribution through simulation and using them for training and test data. Additionally, the result of this experiment has not been quantitatively evaluated. It will be necessary to quantitatively evaluate the classification accuracy.

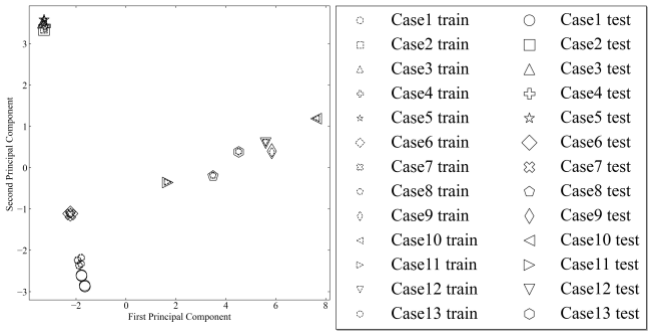

Figure 6(a). The scatter plot of 2-dimension feature space by PCA.

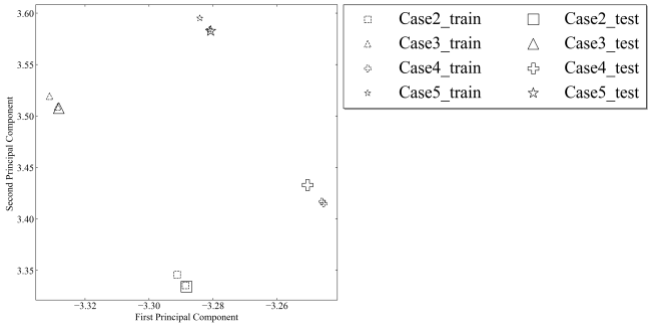

Figure 6(b). Result of reconstruction error for each cases using PCA, SV fault.

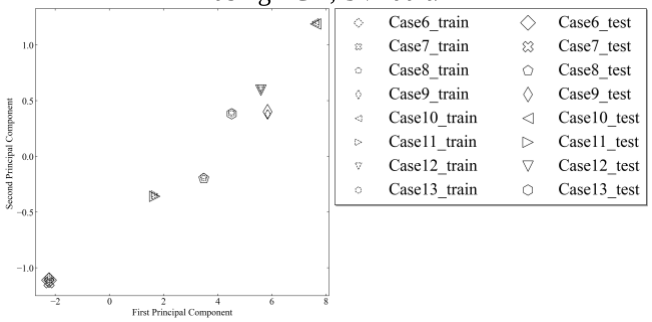

Figure 6(c). Result of reconstruction error for each cases using PCA, bubble anomaly.

6. CONCLUSION

In this study, a method for fault diagnosis using Principal Component Analysis (PCA) , feature extraction for its input, and feature optimization using the greedy algorithm is proposed. The effectiveness of this method was evaluated using data generated from a physical simulation model of a spacecraft propulsion system. By comparing the PCA reconstruction error between normal data and the target data, it was demonstrated that fault detection is possible. Additionally, it was demonstrated that by reducing the high-dimensional data to two dimensions using PCA trained with data containing anomalies, identification of abnormal locations and diagnosis of root causes can be achieved by comparing the data clusters with known data. The quantitative evaluation for fault diagnosis has not yet been accomplished, indicating the need to take this aspect into account in future research. The data used in this experiment were generated experimentally, and since the number of data was small, further data generation is planned to create a more accurate model that can handle the various cases. Additionally, since the physical model used in this study is relatively simple, it is necessary to confirm whether this method can be adapted to more realistic spacecraft propulsion system models. Furthermore, when applying this kind of data-driven method on-board, computational cost becomes a significant element. Therefore, it is necessary to measure the execution time using a computer with equivalent performance to those installed on actual spacecraft and evaluate the feasibility of on-board execution.

REFERENCES

Hoang, D. H., & Nguyen, H. D. (2018). A pca-based method for iot network traffic anomaly detection. In 2018 20th international conference on advanced communication technology (icact) (p. 381-386). doi: 10.23919/ICACT.2018.8323

Hundman, K., Constantinou, V., Laporte, C., Colwell, I., & Soderstrom, T. (2018). Detecting spacecraft anomalies using lstms and nonparametric dynamic thresholding. In Proceedings of the 24th acm sigkdd international conference on knowledge discovery amp; data mining (p. 387–395). New York, NY, USA: Association for Computing Machinery. Retrieved from https://doi.org/10.1145/3219819.3219845 doi: 10.1145/3219819.321

Kawatsu, K., Noumi, A., Ishihama, N., Nagata, T., Inoue, C., Fujii, G., Daimon, Y. (2020). Resilient redundant spacecraft gn&c system fault detection and diagnostics. In of the aerospace europe conference, aec2.

Khan, S., & Yairi, T. (2018). A review on the application of deep learning in system health management. Mechanical Systems and Signal Processing, 107, 241-265.

Modelica Association, Modelica Language Specification, https://www.modelica.org/documents (accessed April 1, 2023).

Saruta, K., Tsukimori, K., Shimada, Y., Nishimura, A., & Kobayashi, T. (2010). Development of a health monitoring system using thermally stable fiber bragg gratings for fast reactor power plants: Experimental demonstration of strain measurement. JAEA Conf , 149-15

SimulationX, https://www.simulationx.com/ (accessed April 1, 2023).

Tominaga, K., Daimon, Y., Toyama, M., Adachi, K., Tsutsumi, S., Omata, N., & Nagata, T. (2023). Dataset generation based on 1D-CAE modeling for fault diagnostics in a spacecraft propulsion system. To be published.

Tominaga, K., Fujii, G., Nagata, T., Wada, D., Hisada, S., Kawatsu, K., & Kasai, T. (2022). Anomaly detection method of spacecraft propulsion using multi- plexed fiber bragg grating. 9th European Conference for Aeronautics and Space Science, https://doi.org/10.13009/EUCASS2022-6177 doi: 10.13009/EUCASS2022-6177

Wold, S., Esbensen, K., & Geladi, P. (1987). Principal component analysis. Chemometrics and intelligent laboratory systems, 2(1-3), 37–52

Yairi, T., Takeishi, N., Oda, T., Nakajima, Y., Nishimura, N., & Takata, N. (2017). A data-driven health monitoring method for satellite housekeeping data based on proba- 4 Asia Pacific Conference of the Prognostics and Health Management Society 2023 bilistic clustering and dimensionality reduction. IEEE Transactions on Aerospace and Electronic Systems, 53(3), 1384-1401. doi: 10.1109/TAES.2017.2